

## THE EFFECTS OF MAGNETIC FIELDS ON RADIATIVE COOLING JETS

E. M. de Gouveia Dal Pino and A. H. Cerqueira

Instituto Astronômico e Geofísico, IAG-USP, São Paulo

### RESUMEN

Revisamos los resultados de estudios recientes de los efectos de campos magnéticos sobre la estructuras y la evolución de jets estacionarios y pulsados superdensos con enfriamiento, que se realizaron con la ayuda de simulaciones MHD tridimensionales. Se consideran tres topologías iniciales del campo magnético: (i) helicoidal y (ii) longitudinal, que ambos permean el jet y el medio ambiente, y (iii) un campo puramente toroidal en el jet. Usando un conjunto de parámetros que es particularmente adecuado para jets protoestelares, examinamos la estructura de emisión de los nodos internos y la superficie de trabajo delantera y comparamos con una base no magnética como también con cálculos 2-D MHD.

### ABSTRACT

We here review the results of recent studies of magnetic field effects on the structure and evolution of overdense, radiatively cooling, steady and pulsed jets, which were carried out with the help of fully three-dimensional MHD simulations. Three initial magnetic field topologies are considered: (i) a helical and (ii) a longitudinal field, both of which permeate the jet and the ambient medium, and (iii) a pure toroidal field in the jet. Using a set of parameters that is particularly appropriate to protostellar jets, we examine the emission structure of the internal knots and the leading working surface, comparing our results with a nonmagnetic baseline and also with 2-D MHD calculations.

*Key Words:* **MAGNETOHYDRODYNAMICS — ISM: JETS AND OUTFLOWS — STARS: PRE-MAIN-SEQUENCE**

### 1. INTRODUCTION

Low-mass young stellar objects produce collimated optical outflows (the Herbig-Haro, hereafter HH, jets) that may extend from a few 1000 AU to very large parsec-length scales, and have embedded in them bright emission-line knots which are radiating shock fronts propagating with velocities of a few hundred km s<sup>-1</sup> into the ambient medium (e.g., Bally & Reipurth 2002, these proceedings).

It has been known for some time that the dynamics of these jets is very much affected by radiative cooling due to the recombination of the shock-excited gas, since the typical cooling times behind the shocks, which do not exceed a few hundred years, are much smaller than the dynamical time scales of these jets,  $t_{\text{dyn}} = R_j/v_j \simeq 10^4$  to  $10^5$  yr (where  $R_j$  is the jet radius, and  $v_j$  its velocity). The importance of the cooling on the jet dynamics has been confirmed by extensive hydrodynamical numerical work (e.g., Blondin et al. 1990; de Gouveia Dal Pino & Benz 1993, Stone & Norman 1993; see also Reipurth & Raga 1999; Cabrit, Raga, & Gueth 1997 for reviews).

Another aspect that seems to play a major role, both in the production and collimation of the HH jets, is the presence of magnetic fields. The most

promising mechanism for their launching involves magneto-centrifugal forces associated either with the accretion disk that surrounds the star (e.g., Königl & Pudritz 2000), or with the disk-star boundary (in the X-winds; e.g., Shu et al. 1994; Shang et al. 2002). In either case, the poloidal field lines that are launched from the star-disk system are expected to wind up like a spring, thus developing a toroidal component that is able to collimate the gas outflow towards the rotation axis. Direct observations of magnetic fields are difficult, and only recently Ray et al. (1997) have obtained the first direct evidence, based on polarization measurements, of  $B \sim 1$  G in the outflow of T Tau S at a distance of few tens of AU from the source. Using magnetic flux conservation and typical jet parameters, this latter result would imply a plasma  $\beta = p_{j,\text{gas}}/(B^2/8\pi) \simeq 10^{-3}$  for a toroidal field configuration, and  $\sim 10^3$ , for a longitudinal field, at distances  $\sim 0.1$  pc. Since ambipolar diffusion does not seem to be able to significantly dissipate them (e.g., Frank et al. 1999), the figures above suggest that magnetic fields may also play a relevant role on the outer scales of the flow.

These pieces of evidence have lately motivated several MHD investigations of overdense,<sup>1</sup> radiative

<sup>1</sup>Observations suggest that HH jets are denser than the

cooling jets, in a search for possible signatures of magnetic fields on the large scales of the HH outflows. These studies have been carried out with the help of multidimensional numerical simulations both in two-dimensions (2-D) (Frank et al. 1998, 1999, 2000; Lery & Frank 2000; Gardiner et al. 2000; Stone & Hardee 2000; Gardiner & Frank 2000; O’Sullivan & Ray 2000), and in three-dimensions (3-D) (de Gouveia Dal Pino & Cerqueira 1996; Cerqueira, de Gouveia Dal Pino, & Herant 1997; Cerqueira & de Gouveia Dal Pino 1999, 2001a, b). In this lecture, we try to review and summarize the main results of these studies.

## 2. NUMERICAL APPROACH

The several models above solve the ideal MHD conservation equations employing different numerical techniques (the 2-D calculations have used grid-based codes, while the 3-D models an SPH code; see the references above for details). Most, simply assume a fully ionized (Hydrogen) gas with an ideal equation of state, and a radiative cooling rate (due to collisional de-excitation and recombination behind the shocks) given by the coronal cooling function tabulated for the interstellar gas (e.g., Dalgarno & McCray 1972). O’Sullivan & Ray (2000), in particular, have also included in their model the cooling function for the  $H_2$  molecule.

Given the present uncertainties related to the real orientation and strength of the magnetic field in protostellar jets, three different initial magnetic field configurations have been adopted in most of the models with the  $\beta$  parameter typically varying between  $\beta \simeq 0.1 \rightarrow \infty$ . One of the adopted configurations was an initially constant longitudinal magnetic field parallel to the jet axis permeating both, the jet and the ambient medium,  $\vec{B} = (B_0, 0, 0)$  (e.g., Cerqueira et al. 1997). Another adopted geometry was a force-free helical magnetic field, which also extends to the ambient medium (see, e.g., Fig. 1 of Cerqueira & de Gouveia Dal Pino 1999). In this case, the maximum strength of the magnetic field in the system corresponds to the magnitude of the longitudinal component of the field at the jet axis. The third geometry adopted was a purely toroidal magnetic field permeating the jet only (see, e.g., Fig. 1 of Stone & Hardee 2000). The field in this case is zero on the jet axis, achieves a maximum strength at a radial position in the jet interior (e.g.,  $R_m \simeq 0.9R_j$ ), and returns to zero at the jet surface. This field corresponds to a uniform current density inside the jet

surrounding ambient medium, with number density ratios  $1 < \eta \lesssim 10$ .

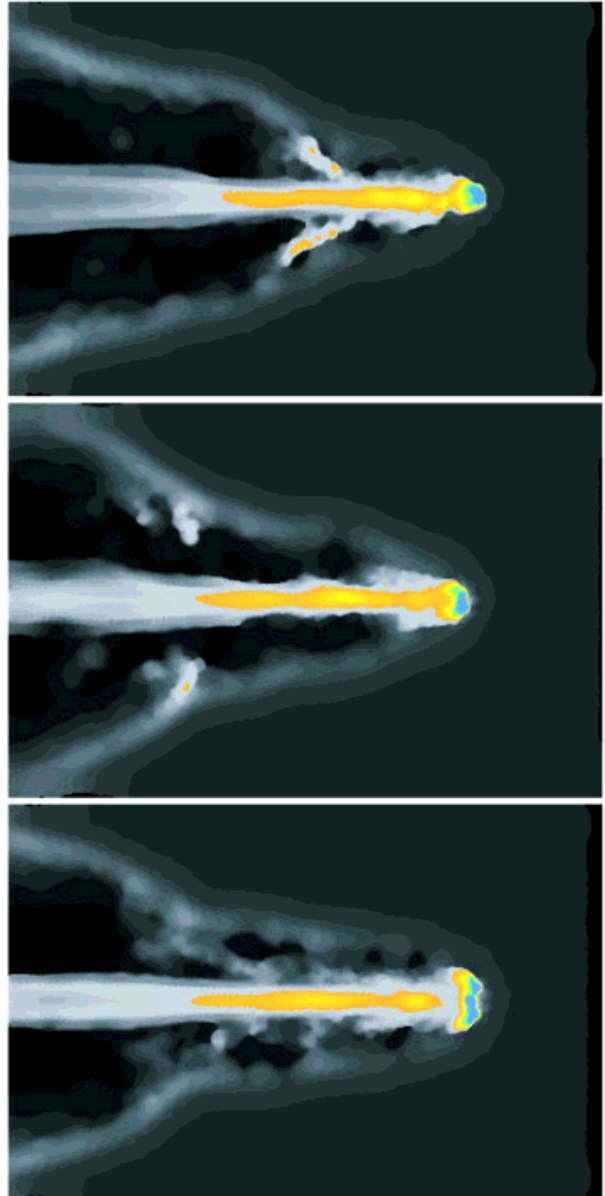


Fig. 1. Gray-scale representation of the midplane density of the head of a hydrodynamical jet (top); an MHD jet with initial longitudinal magnetic field configuration (middle); and an MHD jet with initial helical magnetic field configuration (bottom), at a time  $t/t_d = 1.65$  ( $t_d = R_j/c_a \simeq 38$  years, where  $c_a$  is the ambient sound speed). The initial conditions are:  $\eta = n_j/n_a = 3$ ,  $n_a = 200 \text{ cm}^{-3}$ , average ambient Mach number  $M_a = v_j/c_a = 24$ ,  $v_j \simeq 398 \text{ km s}^{-1}$ ,  $q_{bs} \simeq 8$  and  $q_{js} \simeq 0.3$ . The initial  $\beta = 8\pi\rho/B^2$  for the MHD cases is  $\beta \simeq 1$ . The gray scale (from minimum to maximum) is given by: black, grey, and white. The maximum density reached by the shell at the head of the jets is  $n_{sh}/n_a \simeq 210$  (top),  $n_{sh}/n_a \simeq 153$  (middle), and  $n_{sh}/n_a \simeq 160$  (bottom) (from Cerqueira, et al. 1997).

and a return current at the surface of the jet. In the first two magnetic field configurations, the jet is assumed to have an initially constant gas pressure ( $p_j$ ). In the toroidal configuration, in order to ensure an initial magnetostatic equilibrium, the jet gas pressure has a radial profile with a maximum at the jet axis (Stone & Hardee 2000).

### 3. NUMERICAL RESULTS FOR STEADY-STATE JETS

Let us first briefly review the results for steady jets, that is, jets that are injected with a constant velocity into the ambient medium.

Figure 1 compares 3-D simulations of two MHD jets with initial  $\beta \simeq 1$  (the middle jet has an initial constant longitudinal magnetic field, and the bottom jet has an initial helical magnetic field) with a pure hydrodynamical jet (top panel). At the head, a double shock structure develops with a forward bow shock that accelerates the ambient medium and a reverse jet shock that decelerates the jet material coming upstream. As found in previous numerical HD work, the cooling of the shocked gas at the head results in most of the shocked gas collecting in a dense, cold shell that eventually fragments due to a combination of non-uniform cooling and Rayleigh-Taylor (R-T) instabilities (see the HD jet on the top panel). In the MHD jet with an initially longitudinal field this fragmentation still occurs. In the jet with an initially helical field, on the other hand, the amplification of the toroidal component of the magnetic field reduces the shock compressibility and the growth of the R-T instability, thus inhibiting the shell-fragmentation. This result could be an indication that the latter configuration should dominate near the jet head, as the observed jets have a clumpy structure there (Cerqueira et al. 1997). However, this result is modified in the case of pulsed jets, as we discuss below.

For any geometry, the presence of magnetic fields always tend to improve jet collimation in comparison to purely hydrodynamic calculations. This is due to the amplification and reorientation of the magnetic field components in the shocks, particularly for a helical and a toroidal geometry (e.g., Cerqueira et al. 1997; Cerqueira & de Gouveia Dal Pino 1999; Frank et al. 1998; Stone & Hardee 2000). Longitudinal magnetic fields of different strengths (tested for  $\beta \simeq 0.1-10^7$ ), on the other hand, do not strongly affect the global characteristics of the flow. This occurs because these fields, being predominantly perpendicular to the shock fronts, are not greatly compressed in the shocks and, therefore, the hydrodynamical

forces will always dominate in these cases. However, they do tend to increase order and inhibit instabilities in the flow (Gardiner et al. 2000; O'Sullivan & Ray 2000; Cerqueira & de Gouveia Dal Pino 1999).

For typical HH jet parameters, the multidimensional simulations also indicate the development of MHD Kelvin-Helmholtz *pinch* instabilities along the flow (see Fig. 1), but these pinches are, in general, so weak that it is unlikely that they could play an important role in the formation of the bright emission knots (e.g., Cerqueira & de Gouveia Dal Pino 1999; Stone & Hardee 2000). Pure hydromagnetic pinches have been also detected in simulations involving purely toroidal fields. These can be particularly strong in the presence of intense fields, for example, close to the jet source (e.g., Frank et al. 1998).

### 4. NUMERICAL RESULTS FOR PULSED JETS

The bright emission knots immersed in the HH jets are one of their most prominent features. They frequently exhibit a bow shock morphology and high spatial velocity (e.g., Bally & Reiputh 2001, these proceedings) which indicate that they are shocks that arise from the steepening of velocity (and/or density) fluctuations in the underlying, supersonic outflow. Strong support for this conjecture has been given by theoretical studies which have confirmed that traveling shocks created in this way reproduce the essential properties of the observed knots (e.g., Raga et al. 1990; Kofman & Raga 1992; Stone & Norman 1993; de Gouveia Dal Pino & Benz 1994; Völker et al. 1999; Raga & Cantó 1998; de Gouveia Dal Pino 2001).

To simulate a pulsing jet, it is usually applied a sinusoidal velocity variation with time at the inlet:  $v_0(t) = v_j[1 + A \sin(2\pi t/P)]$ , where  $v_j$  is the mean jet speed,  $A$  the amplitude of the velocity oscillation, and  $P$  the oscillation period.

2-D axisymmetric calculations of pulsed jets show that the presence of toroidal magnetic fields may cause dramatic effects on pulsed jets depending on the initial conditions. For example, Stone & Hardee (2000) have found that the radial hoop stresses due to the toroidal field confine the shocked jet material in the internal pulses, resulting in higher densities in the pulses, which are strongly peaked towards the jet axis in comparison with purely hydrodynamic calculations. O'Sullivan & Ray (2000), on the other hand, carrying out 2-D calculations of jets with initially lower densities (corresponding to a density ratio between the jet and the ambient medium  $\eta = 1$ ), and which are highly overpressurized with respect to the

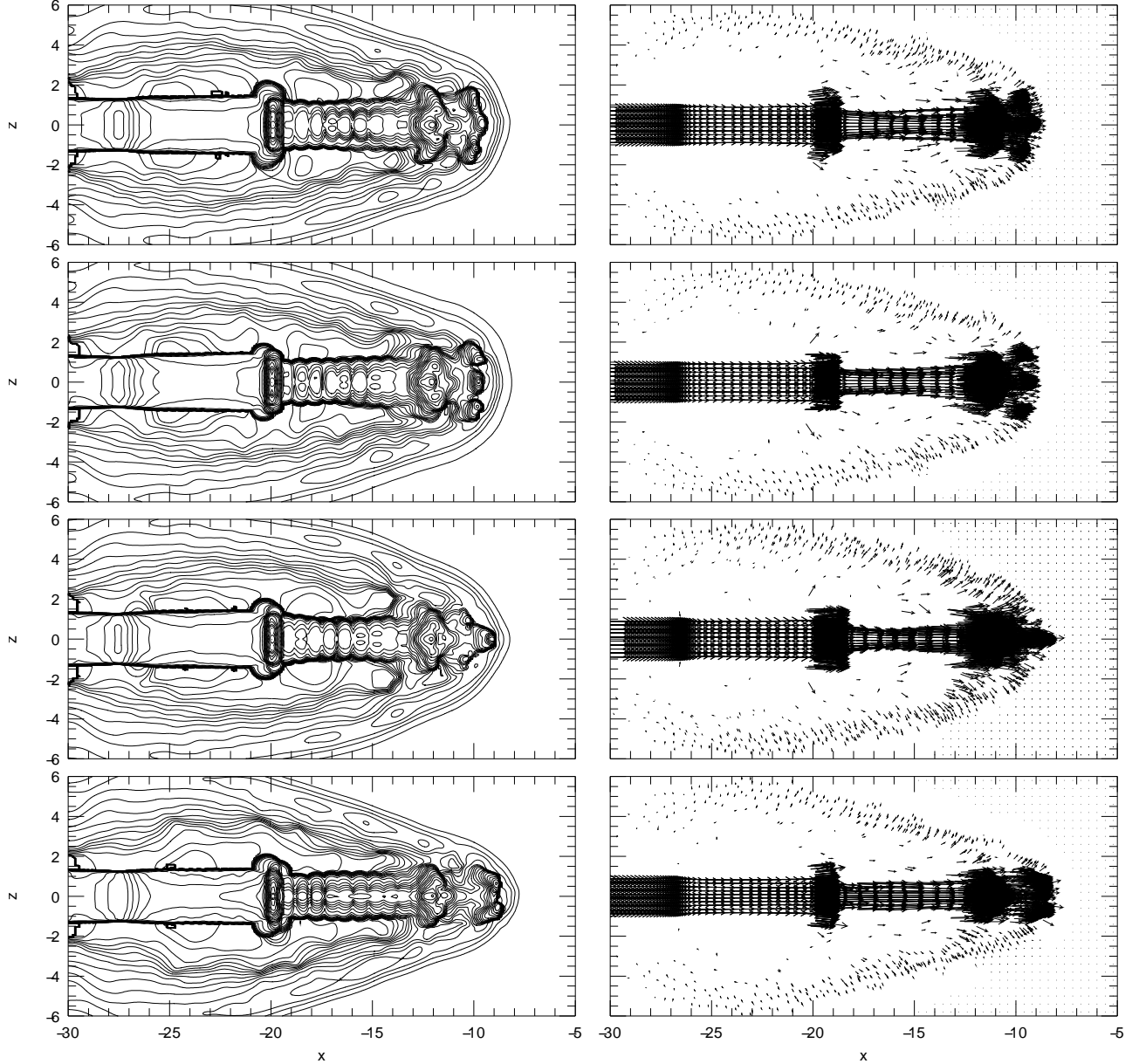


Fig. 2. Midplane density contours (left) and distribution of velocity vectors (right) for (from top to bottom): a purely hydrodynamical pulsed jet; an MHD jet with initial longitudinal magnetic field; an MHD jet with initial helical magnetic field; and an MHD jet with initial toroidal magnetic field, at a time  $t/t_d = 1.75$ . The initial conditions are: average ambient Mach number  $M_a = v_j/c_a \simeq 15$ ,  $v_0 = v_j[1 + A\sin(2\pi t/P)]$ , with  $v_j \simeq 250 \text{ km s}^{-1}$ ,  $A = 0.25v_j$  and  $P = 0.54t_d$ ,  $\eta = n_j/n_a = 5$ ,  $\beta = 8\pi p/B^2 = \infty$  for the HD model, and maximum  $\beta \simeq 1$  for the MHD models. The maximum density in each model (from top to bottom) is: 119, 115, 124 and 175 (1 c.u. =  $200 \text{ cm}^{-3}$ ) (from Cerqueira & de Gouveia Dal Pino 2001a).

ambient medium, find the development of more complex cocoons around the beams and the formation of crossing shocks which help to refocus the beam and the internal pulses. In particular, they find that the hoop stresses associated with toroidal fields can cause a high degree of H ionization and  $\text{H}_2$  dissociation, and the *disruption* of the internal knots, even

for  $\beta \simeq 1$ . Also, in these 2-D models, *nose cones* are found to develop at the head of magnetized jets with toroidal components. These features are extended narrow plugs that form as most of the shocked cooled gas between the jet shock and the bow shock at the head is prevented from escaping sideways into the cocoon (and confined towards the jet axis) by the

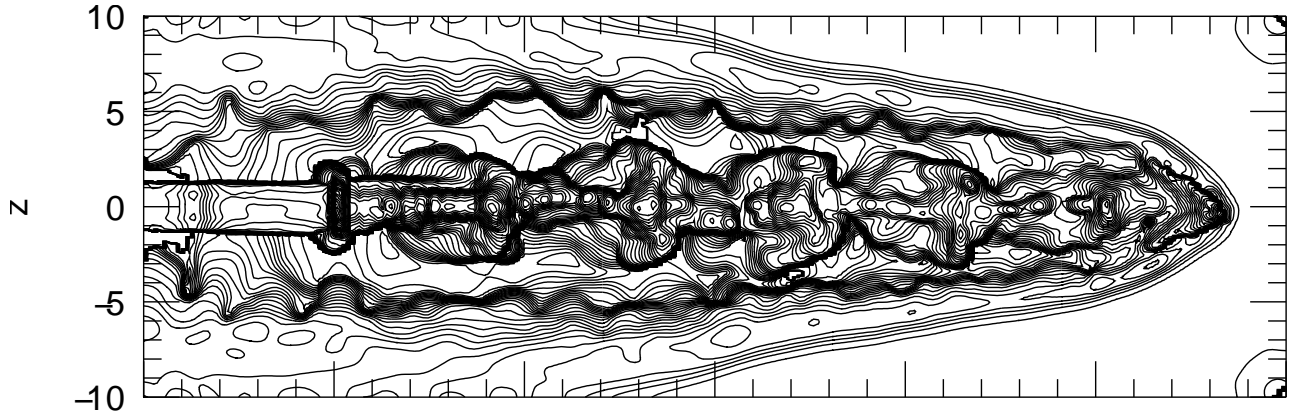


Fig. 3. Midplane density contours for the MHD jet of Fig. 2 with initial helical magnetic field at a time  $t/t_d = 5$  (from Cerqueira & de Gouveia Dal Pino 2001b).

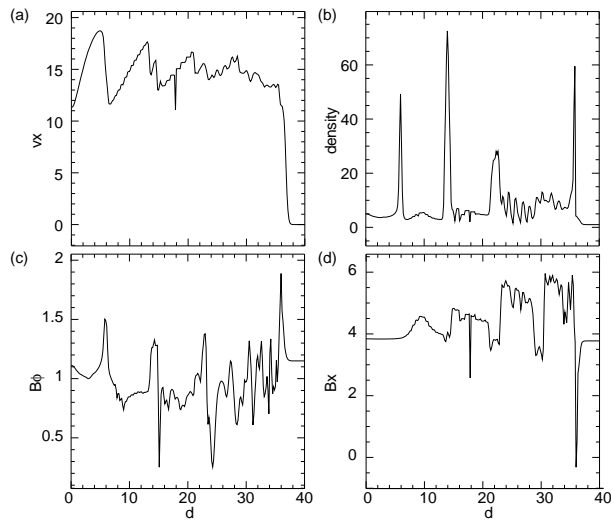


Fig. 4. (a) Velocity, (b) density, (c) toroidal magnetic field component, and (d) longitudinal magnetic field profiles along the beam axis for the jet of Fig. 2 with initial helical magnetic field. Time displayed  $t/t_d \simeq 3$ . (From Cerqueira & de Gouveia Dal Pino 2001a).

toroidal field.

Now, 3-D MHD calculations of pulsed jets reveal significant changes relative to the 2-D models. The morphological features tend to be generally smoothed out in 3-D, and the differences that arise in 2-D calculations with distinct field geometries seem to diminish in the 3-D models (Cerqueira & de Gouveia Dal Pino 2001a,b). As an example, Figure 2 displays the midplane density contours (left) and the velocity field distribution (right), for four supermagnetosonic, radiatively cooling, *pulsed* jets in their early evolution, after they have propagated over a distance  $\approx 22R_j$  (where  $R_j$  is the jet radius). The top jet is purely hydrodynamical (HD), the second

jet has an initial constant longitudinal magnetic field configuration; the third an initial helical magnetic field, and the bottom an initial toroidal field. At the time depicted, the leading *working surface* at the jet head is followed by 2 other features and a third pulse is just entering into the system. Like the leading working surface, each internal feature consists of a double-shock structure, an upstream reverse shock that decelerates the high velocity material entering the pulse, and a downstream forward shock sweeping up the low velocity material ahead of the pulse. At this time, none the internal working surfaces (IWS) or knots has yet reached the jet head. Later on, however, each reaches the terminal working surface one by one and is disrupted by the impact. Their debris are partially deposited into the cocoon, thus drastically changing the head morphology and providing a complex fragmented structure, as in Figure 3, where the jet of Fig. 2 with initial helical field is depicted at a later time of its evolution. No nose cones have developed, not even in the jet with initial toroidal field. We speculate that their absence in the 3-D calculations could be partially explained by the fact that the magnetic forces are intrinsically three-dimensional and so cause part of the material to be deflected in a third direction, thereby smoothing out the strong focusing of the shocked material that is otherwise detected in the 2-D calculations (Cerqueira & de Gouveia Dal Pino 2001a; Stone & Hardee 2000 have also argued that nose cones should be unstable in 3-dimensions).

Fig. 2 also indicates that the overall morphology of the 3-D pulsed jet is not very much affected by the presence of the different magnetic field configurations when compared to the purely HD calculation. Instead, the distinct  $\mathbf{B}$ -profiles tend to alter only the detailed structure behind the shocks at the

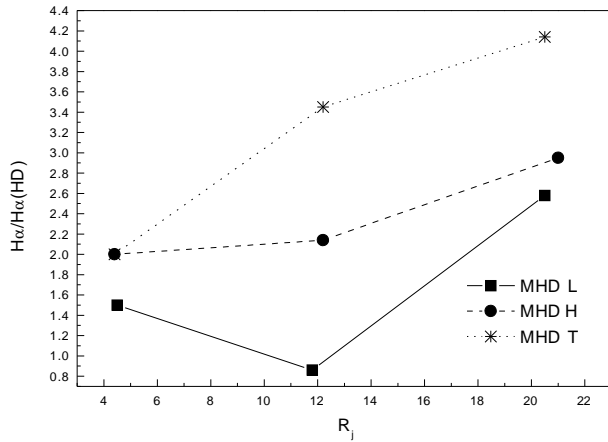


Fig. 5. The ratio between the  $H\alpha$  intensity along the jet axis within the IWSs for the different magnetized jets of Fig. 2 and the  $H\alpha$  intensity of the purely hydrodynamical jet. (from Cerqueira & de Gouveia Dal Pino 2001a).

head and internal knots, particularly in the helical and purely toroidal cases. Like in steady calculations, the pure HD jet exhibits a cold dense shell at the head, formed by the cooling of the shock-heated material, that has also become R-T unstable and separated into clumps. Again, these can also be identified in the shell of the MHD jet with initial longitudinal field, but not in the helical or the toroidal cases. The 3-D simulations also show, as in previous work (e.g., de Gouveia Dal Pino & Benz 1993), that the density of the shell (and IWSs) undergoes oscillations with time (with a period of the order of the cooling time behind the shocks), which are caused by global thermal instabilities of the radiative shocks. The profile and maximum amplitude of these oscillations are particularly affected by the presence of toroidal field components (Cerqueira & de Gouveia Dal Pino 2001b).

Some wiggling can be detected in the jet axis in the 3-D MHD simulation with initial helical field of Figure 3. This is caused by the *kink* mode of the K-H instability and was also detected (but with smaller amplitude) in the pure hydrodynamical counterpart. This could provide a potential explanation for the wiggling features often detected in HH jets.

Several physical quantities along the beam axis of the jet of Fig. 3 with initial helical magnetic field are depicted in Fig. 4, at a time  $t/t_d \simeq 3$ , when two more pulses have entered the system and developed new IWSs, and the first IWS has already merged with the jet head. The initial sinusoidal velocity profile applied to the flow at the inlet steepens into the sawtooth pattern (top panel) familiar from

earlier studies of oscillating jets (e.g., Raga & Kofman 1992) as the faster material catches up with the slower, upstream gas in each pulse. The sharp density spikes within each IWS (second panel) are correlated with the toroidal component of the magnetic field. The third panel shows that this component  $B_\phi$  (third panel) sharpens within the knots and rarefies between them, while the longitudinal component,  $B_\parallel$  (fourth panel) is stronger between the knots (Cerqueira & de Gouveia Dal Pino 2001a). This result is in agreement with 2-D calculations (Gardiner & Frank 2000; O’Sullivan & Ray 2000) and could, in principle, be checked observationally as a diagnostic of helical geometries. Helical fields are specially attractive for protostellar jets as they are the predicted geometry from magneto-centrifugally launched models (Gardiner & Frank 2000; Lery & Frank 2000).

Although the distinct  $\mathbf{B}$ -geometries do not seem to significantly affect the global characteristics of the 3-D flows, they can modify the details of the emission structure, particularly for the helical and toroidal cases. In particular, Figure 5 shows the  $H\alpha$  intensity along the jet axis evaluated within the IWSs for the different magnetized jets of Fig. 2 which are compared to the  $H\alpha$  intensity of the baseline hydrodynamical jet. The  $H\alpha$  intensity is observed to be strong behind the knots of the protostellar jets and is predicted to have a strong dependence with the shock speed  $v_s$ ,  $I_{H\alpha} \propto \rho_d v_s^{3.8}$  where  $\rho_d$  is the downstream pre-shock density (e.g., Raga & Cantó 1998). We have used this relation and the results of the simulated jets of Fig. 2 to evaluate the intensity ratios of Fig. 4. We note, as expected, that the intensity ratio does not differ much from unity in the case of the magnetized jet with initial longitudinal field, while for the helical and toroidal field cases, the  $H\alpha$  intensity can be about four times larger (for  $\beta \simeq 1$  jets) than that of the HD case.

## 5. CONCLUSIONS

The effects of magnetic fields are dependent on both the field-geometry and intensity (which, unfortunately, are still poorly determined from observations). The presence of a helical or a toroidal field tends to affect more the characteristics of the fluid, compared to the purely HD calculation, than a longitudinal field. However, the relative differences which are detected in 2-D simulations involving distinct magnetic field geometries (e.g., Stone & Hardee 2000; O’Sullivan & Ray 2000), seem to decrease in the 3-D calculations (Cerqueira & de Gouveia Dal Pino 2001a,b). In particular, we have found that features, like the nose cones, that often develop at the

jet head in 2-D calculations involving toroidal magnetic fields, are absent in the 3-D models (Cerqueira & de Gouveia Dal Pino 1999, 2001a,b), a result which is consistent with observations which show no direct evidence for nose cones at the head of protostellar jets.

In 3-D calculations, magnetic fields which are initially nearly in equipartition with the gas tend to affect essentially the detailed structure behind the shocks at the head and internal knots, mainly for the helical and toroidal topologies. In such cases, the  $H_\alpha$  emissivity behind the internal knots can increase by a factor up to four relative to that in the purely hydrodynamical jet (Cerqueira & de Gouveia Dal Pino 2001a).

Further 3-D MHD studies are still required as the detailed structure and emission properties of the jets seem to be sensitive to multidimensional effects when magnetic forces are present. Also obvious is the need for further observations and polarization mapping of star formation regions, for a real comprehension of the magnetic field structure of protostellar jets.

Financial support for this research has been provided by the Brazilian agencies FAPESP and CNPq.

#### REFERENCES

- Bally, J., & Reipurth, B. 2002, *RevMexAA(SC)*, 13, 1 (this volume)
- Blondin, J. M., Fryxell, B. A., & Königl, A. 1990, *ApJ*, 360, 370
- Cabrit, S., Raga, A. C., & Gueth, F. 1997, in *IAU Symp. 182, Herbig-Haro Flows and the Birth of Low Mass Stars*, eds. B. Reipurth & C. Bertout (Dordrecht: Kluwer), 163
- Cerqueira, A. H., & de Gouveia Dal Pino, E. M. 1999, *ApJ*, 510, 828
- \_\_\_\_\_. 2001a, *ApJ*, 550, L91
- \_\_\_\_\_. 2001b, *ApJ*, 560, 779
- Cerqueira, A. H., de Gouveia Dal Pino, E. M., & Herant, M. 1997 *ApJ*, 489, L185
- Dalgarno, A., & McCray, R. A. 1972, *ARA&A*, 10, 375
- de Gouveia Dal Pino, E. M. 2001, *ApJ*, 551, 347
- de Gouveia Dal Pino, E. M., & Benz, W. 1993, *ApJ*, 410, 686
- \_\_\_\_\_. 1994, *ApJ*, 435, 261
- de Gouveia Dal Pino, E. M., & Cerqueira, A. H. 1996, *Astron. Lett.*, 34, 303
- Frank, A., Gardiner, T., Delemarter, G., Lery, T., & Betti, R. 1999, *ApJ*, 524, 947
- Frank, A., Lery, T., Gardiner, T., Jones, T. W., & Ryu, D. 2000, *ApJ*, 540, 342
- Frank, A., Ryu, D., Jones, T. W., & Noriega-Crespo, A. 1998, *ApJ*, 494, L79
- Gardiner, T. A., & Frank, A. 2000, *ApJ*, 545, L153
- Gardiner, T. A., Frank, A., Jones, T. W., & Ryu, D. 2000, *ApJ*, 530, 834
- Königl, A., & Pudritz, R. E. 2000, in *Protostars and Planets IV*, Eds. V. Mannings, A. Boss & S. Russell (Tucson: Univ. Arizona Press), 759
- Kofman, L., & Raga, A. C. 1992, *ApJ*, 390, 359
- Lery, T., & Frank, A. 2000, *ApJ*, 533, 897
- O'Sullivan, S., & Ray, T. P. 2000, *A&A*, 363, 355
- Raga, A. C., & Cantó, J. 1998, *RevMexAA*, 34, 73
- Raga, A. C., Cantó, J., Binette, L., & Calvet, N. 1990, *ApJ*, 364, 601
- Raga, A. C., & Kofman, L. 1992, *ApJ*, 386, 222
- Ray, T. P., Muxlow, T. W. B., Axon, D. J., Brown, A., Corcoran, D., Dyson, J., & Mundt, R. 1997, *Nature*, 385, 415
- Reipurth, B., & Raga, A. C. 1999, in *The Origin of Stars and Planetary Systems*, Eds. C. J. Lada & N. D. Kylafis (Dordrecht: Kluwer), 267
- Shang, H., Glassgold, A. E., Shu, F. H., & Lizano, S. 2002, *ApJ*, 564, 853.
- Shu, F. H., Najita, J., Ostriker, E., Wilkin, F., Ruden, S. P., & Lizano, S. 1994, *ApJ*, 429, 781
- Stone, J. M., & Hardee, P. E. 2000, *ApJ*, 540, 192
- Stone, J. M., & Norman, M. L. 1993, *ApJ*, 413, 198
- Völker, R., Smith, M. D., Suttner, G., Yorke, H. W. 1999, *A&A*, 345, 953

E. M. de Gouveia Dal Pino and A. H. Cerqueira: Instituto de Astronômico e Geofísico, Universidade de São Paulo, Caixa Postal 3386, 01060-970 São Paulo, SP, Brazil (dalpino,adriano@iagusp.usp.br).